Synthesis of Zeolite from Coal Fly Ash by Hydrothermal Method Without Adding Alumina and Silica Sources: Effect of Aging Temperature and Time

(Sintesis Zeolit daripada Abu Cerobong Arang Batu melalui Kaedah Hidroterma
Tanpa Menambah Sumber Alumina dan Silika: Kesan Penuaan Suhu dan Masa)

W. Chansiriwat, D. Tanangteerapong & K. Wantala*

ABSTRACT

The aim of this research was to synthesize zeolite from coal fly ash by hydrothermal method. The effect of aging temperature and time on zeolite P1 synthesis (Na-P1) from Mae Moh coal fly ash (MFA) without adding any alumina and silica sources were examined during the synthesized process. The central composite design (CCD) was used for experimental design to obtain the optimal process parameters of the aging temperature (105-195ºC) and time (12-84 h) where the specific surface area was used as a response. The chemical and physical properties of Na-P1 such as specific surface area, crystalline phase, compositions and morphology were examined. The response results showed that the specific surface area of Na-P1 decreased with an increase of both aging temperature and time, whereas the XRD intensity of Na-P1 increased with an increase of both aging temperature and time. The composition of SiO_2/Al_2O_3 in mass ratio of coal fly ash was observed, which was suitable to Na-P1 synthesis. The maximum specific surface area of zeolite products was found at the designed condition of aging temperature of 105ºC and time of 12 h. Thus, zeolite P1 can be prepared by hydrothermal method without adding any alumina and silica sources.

Keywords: Coal fly ash; Coal power plant; response surface methods; zeolite synthesis

ABSTRAK

Tujuan kajian ini adalah untuk mensintesis zeolit daripada abu cerobong arang batu melalui kaedah hidroterma. Kesan penuaan suhu dan masa pada zeolite sintesis P1 (Na-P1) daripada abu cerobong arang batu Mae Moh (MFA) tanpa menambah apa-apa sumber alumina dan silika dikaji semasa proses sintesis. Pusat reka bentuk komposit (CCD) telah digunakan untuk uji kaji reka bentuk bagi mendapatkan parameter proses optimum pada suhu penuaan (105-195ºC) dan masa (12-84 h) dengan kawasan permukaan tertentu digunakan sebagai tindak balas. Sifat kimia dan fizikal Na-P1 seperti kawasan permukaan yang khusus, fasa hablur, komposisi dan morfologi telah ditentukan. Hasil maklum balas menunjukkan bahawa kawasan permukaan tertentu Na-P1 menurun dengan peningkatan suhu penuaan dan masa, manakala keamatan XRD Na-P1 terus meningkat dengan peningkatan suhu penuaan dan masa. Komposisi oleh SiO_2/Al_2O_3 dalam nisbah jisim abu cerobong arang batu diperhatikan, sesuai untuk sintesis Na-P1. Kawasan maksimum permukaan tertentu produk zeolit telah ditemui pada satu keadaan penuaan suhu 105ºC dan masa 12 h. Oleh itu, zeolit P1 boleh disediakan dengan menggunakan kaedah hidroterma tanpa menambah apa-apa sumber alumina dan silika.

Kata kunci: Abu cerobong arang batu; kaedah gerak balas permukaan; loji janakuasa arang batu; sintesis zeolit

INTRODUCTION

Coal is the most plentiful fuel resource among other fossil fuel and can also be found everywhere in the world (Izidoro et al. 2012). This fuel was generally used in coal power plant to produce the electricity. Fly ash is one of the by-products emitting by the coal power plant. Currently, fly ash is used in the construction industry by mixing it with the alkaline solution to produce geopolymer cement which has higher quality than conventional cement (Ma et al. 2016; Onutai et al. 2015; Okoye et al. 2015; Phoo-Ngernkham et al. 2015). Moreover, it is an inexpensive material because it is a type of waste generated from the thermal power plant. Generally, fly ash was used as a precursor in zeolite synthesis because it contains high silica and alumina contents. Thus, fly ash is possible to

use as raw material in zeolite synthesis due to the same composition of alumino-silicate (Si and Al) (Thuadaij & Nuntiya 2012). In the middle of 1980, zeolite synthesis had been widely studied by many researchers and still developing until now (Belviso et al. 2015; Bukhari et al. 2015; Cardoso et al. 2015; Grela et al. 2016; Pimraksa et al. 2010; Volli & Purkait 2015; Wei et al. 2015; Zhang et al. 2013b). Mae Moh power plant is one of the coal thermal power plants located in the northern part of Thailand where tons of lignite was used to generate the electricity. Mae Moh fly ash (MFA) is categorized to class C, which contain SiO_2, Al_2O_3 and Fe_2O_3 between 50-70% by weight (ASTM standard). Thuadaij and Nuntiya (2012) synthesized zeolite X from MFA by adding amorphous silica and alumina source from metakaolin to adjust the ratio of Si:

Al to 3.25. Moreover, MFA was synthesized to be zeolite P1 (Na-P1) by hydrothermal treatment at aging time and temperature at about 96 h and 110ºC, respectively (Rongsayamanont & Sopajaree 2007). However, it is currently unclear how the crystallite phase changed to form Na-P1 and the interaction effect between aging time and aging temperature has not yet been reported (Rongsayamanont & Sopajaree 2007). Izidoro et al. (2012) synthesized zeolite from five different sources of coal fly ash generated from the Brazilian coal power plants by hydrothermal treatment at 100ºC and 24 h without adding silica and alumina source using NaOH concentration of 3.5 molar. They reported that different sources of coal fly ash produced different zeolite types. They also reported the mass ratios of SiO_2 to Al_2O_3 in Na-P1 were 1.8 and 2.7. Additionally, Murayama et al. (2002) reported that the quality of zeolite depended on the concentration of alkaline (NaOH) solution which therefore, affected the aging temperature in the process of zeolite synthesis. Kazemian et al. (2010) synthesized Na-P1 from coal fly ash containing high silicon by hydrothermal treatment by adding alumina to increase the Si/Al ratio ($2.2SiO_2$: Al_2O_3: $5.28Na_2O$: $106H_2O$) and using high concentration of NaOH (5.53 molar). They reported the similar conditions to synthesize Na-P at 120ºC but aging time reported in Sang et al. (2006) was longer at 24 h. The aging time reported in Sang et al. (2006) was higher than the one reported in Kazemian et al. (2010) due to lower NaOH concentration was used. Thus, it has conclusively been shown that the NaOH concentration had a significant effect on the aging temperature and time in zeolite synthesis by hydrothermal method. The results reported by Adamczyk et al. (2005) were in agreement with other works, which highlighted that a higher NaOH concentration resulted in a shorter aging time in zeolite synthesis by hydrothermal. However, they argued that fly ash containing high amount of silica, alumina and iron cannot synthesize the pure Na-P1 (Adamczyk & Bialecka 2005). On the other hands, Murayama et al. (2002) reported that the optimal NaOH concentration for Na-P1 synthesis was about 2 to 3 molar. Therefore, it would be interesting to synthesis pure Na-P1 from MFA and to understand the effects of aging temperature and time in zeolite synthesis by hydrothermal method by using low NaOH concentration. Besides, this is the first report regarding the main and interaction effects of both aging temperature and time in hydrothermal process to synthesis Na-P1 from coal fly ash.

In this research, the synthesis of Na-P1 from MFA by hydrothermal method without adding any silica and alumina source using 2.8 molar NaOH concentrations was conducted. The aging temperature and time in hydrothermal conditions were optimized by using central composite design (CCD). The main and interaction effects were evaluated by using mathematics and statistics techniques. The physical and chemical properties were done by using N_2 adsorption-desorption analysis then the specific surface area was calculated by Brunauer-Emmett-

Teller (BET) method, X-ray diffraction (XRD), X-ray florescence spectrometer (XRF) and scanning electron microscopy (SEM).

MATERIALS AND METHODS

CHEMICALS

The sodium hydroxide used in this work was analytical grade (>97%, NaOH, RCL Labscan limited). The MFA was collected from Mae Moh coal power plant located in northern part of Thailand.

ZEOLITE PI SYNTHESIS

Na-P1 was synthesized via hydrothermal method. The central composite design (CCD) was used to design experimental conditions to study the effects of aging temperature by using MiniTab 16 statistical software (Minitab, Inc., Pennsylvania, USA). The Na-P1 synthesis was prepared by the following procedure. Solution A was prepared by mixing 30.25 g of distilled water with 10 g of NaOH and 16.86 g of MFA at 100ºC under vigorous mixing. After that, 10 g of solution A was mixed with 5.61 g of NaOH in 61.20 g of distilled water labeling as seed gel. The composition of seed gel in mole ratio was $3.0SiO_2$: $1.0Al_2O_3$: $16.0Na_2O$: $641.5H_2O$. Solution B was prepared by mixing 75.00 g of distilled water with 8.27 g of NaOH and 7.98 g of MFA at 100ºC under vigorous mixing which is called 'mother gel'. The composition of mother gel in mole ratio was $3.0SiO_2$: $1.0Al_2O_3$: $6.6Na_2O$: $267.7H_2O$. After that, both seed gel and mother gel solutions were mixed together and continuously stirred not less than 30 min. The composition of this mixed gel in mole ratio was $3.0SiO_2$: $1.0Al_2O_3$: $9.2Na_2O$: $368.6H_2O$. Next, the mixing solution was transferred to a Teflon-line placed in the stainless steel autoclave and then aged in an oven at the design conditions as displayed in Table 1. The NaOH concentration in mixed gel was found to be 2.8 molar, which was a suitable NaOH concentration ranging between 2 and 3 molar in order to prepare Na-P1 reported elsewhere (Murayama et al. 2002). Finally, the solid solution was obtained after aging in the oven. After that, it was separated by centrifugal technique. The supernatant liquid was removed and the solid was washed with distilled water until the pH was lower than 9.0 and then dried overnight in an oven at 100ºC.

CHARACTERIZATIONS OF SAMPLES

The characterizations of Na-P1 were carried out by many techniques. For example, the specific surface area was analyzed by N_2 adsorption-desorption instrument (ASAP 2010, Micromeritics, USA) and calculated by Brunauer-Emmett-Teller analytical (BET) technique. The crystalline phase was conducted by X-ray diffraction (XRD) (Model D8 Discover, Bruker AXS, Germany) using Cu Kα with wavelength 1.51418 Å at 40 mA and 40kV with 2θ range of 10-50 degrees and increasing step of 0.02 degree.

TABLE 1. Central composite design (CCD) for varying hydrothermal aging temperature and times

Run	Temperature (ºC)	Time (h)
1	150	48
2	120	24
3	150	48
4	150	48
5	195	48
6	150	12
7	180	72
8	150	48
9	180	24
10	105	48
11	120	72
12	150	48
13	150	84

The proportional compositions of MFA and Na-P1 were measured by X-ray fluorescence (XRF, Bruker AXS, Germany, Model: S4 Pioneer Wavelength dispersive X-Ray Fluorescence (WDXRF) Spectrometry) at 60 kV and 50 mA. The morphologies of the MFA and Na-P1 samples were investigated by using scanning electron microscope (SEM S-3000N, Hitachi, Japan). The specific surface areas were calculated by BET equation, which was used as a response in effect of aging temperature and time. The estimated regression coefficients (β) was computed by least square of error technique and then replace this parameter in full quadratic equation as displayed in (1) to estimate the response (Suwannaruang et al. 2015).

$$Y = \beta_0 + \Sigma_{i=1}^{2} \beta_i X_i + \Sigma_{i=1}^{2} \beta_{ii} X_i^2 + \Sigma_{i=1}^{2} \Sigma_{i \neq j}^{2} \beta_{ij} X_{ij} + \varepsilon, \quad (1)$$

where Y is the responses (specific surface area); X_i and X_j are the parameters in the hydrothermal process which are the aging temperature and time, respectively; β is the regression coefficient value; and ε is the experimental error.

RESULTS AND DISCUSSION

The morphology of MFA was examined by SEM as shown in Figure 1(a). Most of the MFA particles had spherical shapes in various particle sizes and having smooth surfaces covered with some alumino-silicate glass phase reported elsewhere (Izidoro et al. 2012; Murayama et al. 2002; Rongsayamanont & Sopajaree 2007). After MFA was treated with NaOH solutions by hydrothermal in different aging temperature and aging time, it was thought that Na-P1 was synthesized. The results of the obtained particles were observed under SEM as shown in Figure 1(b)-1(f) and found that the small particles of Na-P1 deposits on the surface of fly ash. This is because, the amorphous alumino-silicates in fly ash were dissolved in alkaline solution and formed sodium-silicate and allumino-silicate gels. This process is called the dissolution process which will be used as a precursor to synthesize the zeolite (Murayama et al. 2002).

Continuously, these two gels were aged at the different aging temperature and time before the Na-P1 particles were formed on the surface of spherical MFA. This process is called recrystallization process. The results in Figure 1(b)-1(f) indicates that longer aging time and temperature created thicker particle surfaces. This is due to more deposition of Na-P1 on the MFA surface (Adamczyk & Bialecka 2005; Murayama et al. 2002; Rongsayamanont & Sopajaree 2007). The morphologies of all samples prepared at different aging temperature and time are in agreement with earlier studies (Cama et al. 2005; Murayama et al. 2002; Rongsayamanont & Sopajaree 2007). The morphologies of Na-P1 were prepared in the same aging time at 48 h and different aging temperature at 105ºC, 150ºC and 195ºC were displayed in Figure 1(b), 1(c) and 1(d), respectively. The results found that the more deposits of Na-P1 on spherical MFA increased with increasing of aging temperatures. However, the zeolite on the surface of the particle gradually broke down and thus, the particles became out of spherical shape. In the same way, the morphologies of Na-P1 prepared in the same aging temperature at 150ºC and different aging time at 12, 48 and 84 h were presented in Figure 1(e), 1(c) and 1(f), respectively. Similarly, the more deposits of Na-P1 on spherical MFA increased with increasing of aging times. Thus, it can be concluded that both aging temperature and time had significantly effects on the formation of Na-P1.

The XRD results of crystallite samples before Na-P1 synthesis and after hydrothermal process at different aging temperature and time are shown in Figure 2(a) and 2(b), respectively. The XRD peak of MFA in Figure 2(a) was observed for mullite and hematite which is consistent to the study reported by Adamczyk and Bialecka (2005). The other peaks in this XRD pattern after hydrothermal process were corresponded to the zeolite found in Na-P1 type which was referred to JCPDS 39-0219 standard and other researches (Izidoro et al. 2012; Kazemian et al. 2010; Murayama et al. 2002). Additionally, it can be clearly seen in the XRD patterns that the crystallinity of Na-P1 sample gradually increased with increasing of either aging temperature or aging time. This XRD results are consistent with SEM images which explains the effects of aging temperature and time on the deposition of Na-P1 on the surface morphology. The more dissolubility of alumino-silicate from the surface of MFA to form sodium-silicate and alumino-silicate gels at high aging temperature and longer aging time was observed. After that, the sodium-silicate and alumino-silicate gels were recrystallized to zeolite and re-deposited on the surface which is consistent to the previous SEM images shown in Figure 1(d) and 1(f). Zhang et al. (2013a) also reported that the reaction temperature mainly affects the nucleation process and crystal growth process. Thus, the higher aging temperature can increase the concentration of sodium-silicate and alumino-silicate in the solution which
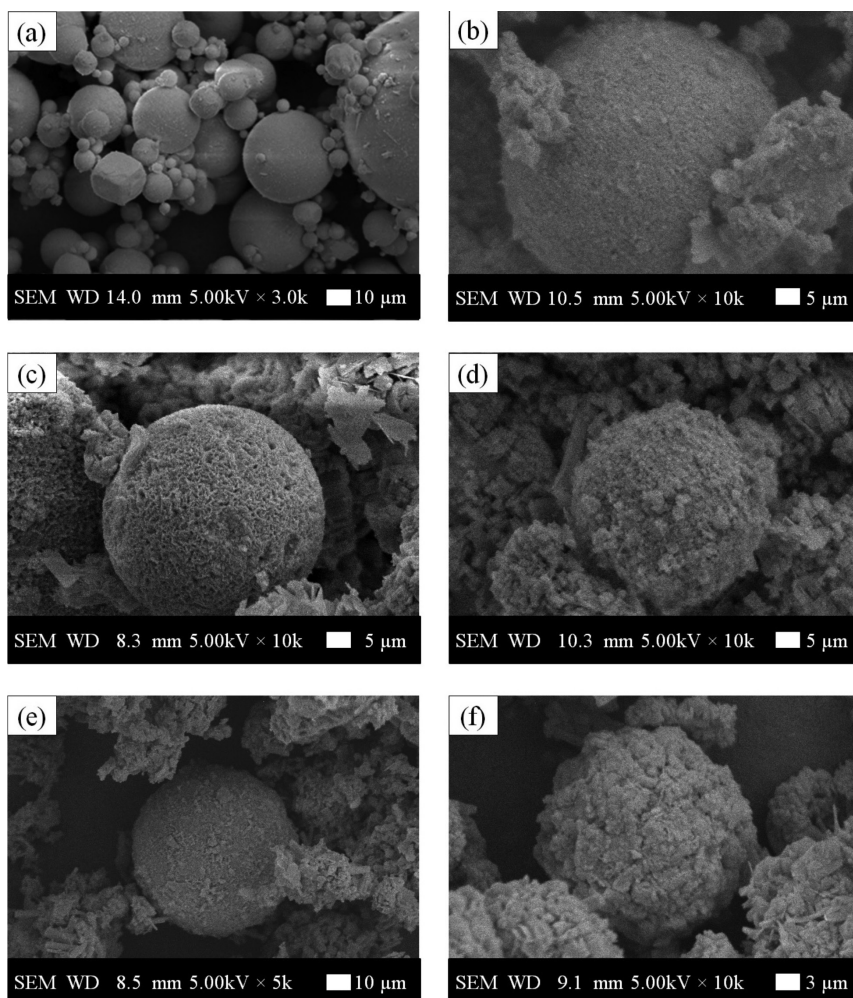
FIGURE 1. SEM morphologies of (a) fly ash and Na-P1 prepared at, (b) 105ºC, 48 h, (c) 150ºC, 48 h,
(d) 195ºC, 48 h, (e) 150ºC, 12 h and (f) 150ºC, 84 h

is very useful for the crystallization process (Zhang et al. 2013a). It can be concluded that sodium-silicate and alumino-silicate gels can produced more at a higher aging temperature and longer aging time. X-ray diffraction peaks of synthesized Na-P1 at low aging temperature and time gradually widen and weaken, which might be the position of the smaller particle size of zeolite samples reported elsewhere (Sang et al. 2006).

Thus, zeolite product will be used as a support material in our further study for $CuFe_2O_3$ loaded over Na-P1 in Fenton-like reaction. Therefore, the specific surface area is a significant parameter to be examined for the support material of this work. The results of specific surface areas in every condition are shown in Table 2. It can be seen that the specific surface area of all Na-P1 samples were higher than that of MFA raw material (0.16 m^2/g). Furthermore, the specific surface areas decreased with increasing of aging temperature and time. This can be confirmed by the SEM and XRD results shown in Figures 1(d) and 2(b) at the aging temperature of 150°C and aging time of 84 h which indicates that all of the

created synthesized zeolite covered on the surface of zeolite P1 and thus, decreasing the specific surface areas to 5.14 m^2/g. The estimated coefficients were calculated by using the least square of error by replacing β in (1). The resulting values are shown in Table 3 and the new (2) was obtained.

$$Y = 18.870 - 8.094X_1 - 7.773 X_2 + 3.778 + 0.4095 - 2.445X_1X_2 \qquad (2)$$

Here, Y is the specific surface area (m^2/g), X_1 and X_2 are coded values of aging temperature and aging time, respectively, X_1X_2 is the interaction between aging temperature and aging time. and are the square terms of aging temperature and aging time, respectively. At 95% confidence, the results showed that both of main effects were significant to surface area in negative effect (P_{Value} < 0.05). The result was related with SEM images because of the covering of Na-P1 on surfaces of spherical shape to cover the pore of materials. This can be implied that the specific surface area decreased with increasing of both
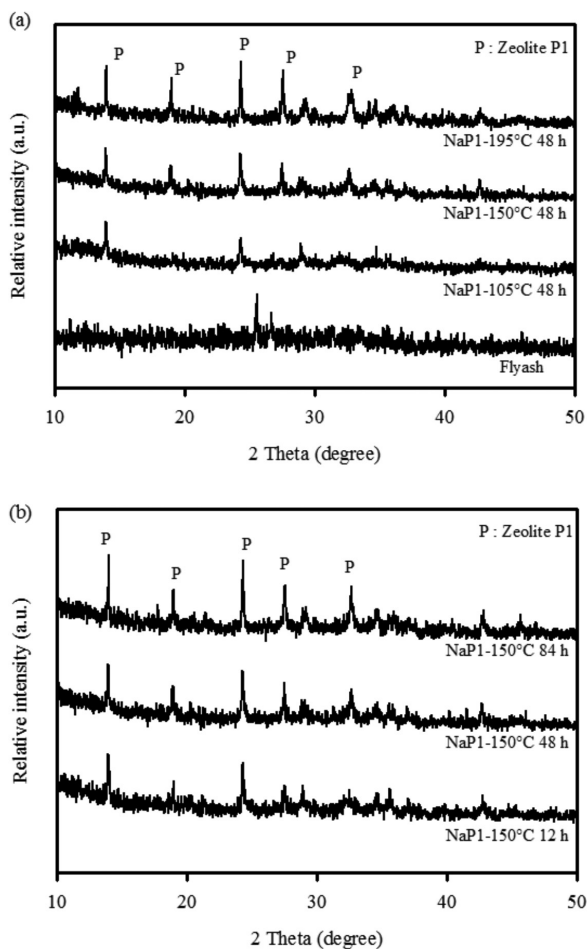
(a)

(b)

FIGURE 2. XRD pattern of (a) MFA and synthesized Na-P1 samples at different aging temperature and (b) synthesized Na-P1 samples at different aging time

TABLE 2. Specific surface area results of zeolite P1 for every run order designed by CCD

Run	Temperature (°C)	Time (h)	Specific surface area (m²/g)
1	150	48	19.05
2	120	24	38.65
3	150	48	18.54
4	150	48	19.99
5	195	48	8.23
6	150	12	27.08
7	180	72	10.86
8	150	48	15.85
9	180	24	32.33
10	105	48	39.15
11	120	72	26.96
12	150	48	19.08
13	150	84	5.14

positive effect to specific surface area as shown in Table 3. Identically, the interaction between aging temperature and aging time was displayed an insignificant effect on specific surface area of Na-P1. In order to confirm the accuracy of experimental results, the standard errors in every run of experiment were used to explain the error of experiments by comparing between predicted results computed by (2) and the experimental results. Figure 3 shows the normal probability plot of residuals, histogram, residuals versus fitted values and residuals

TABLE 3. Estimated regression coefficients (β) for specific surface area

Parameter terms	Coefficients	P-value
Constant	18.870	0.000
Temperature	-8.094	0.002
Time	-7.773	0.003
Temperature * Temperature	3.778	0.071
Time * Time	0.4095	0.824
Temperature * Time	-2.445	0.370

effects in hydrothermal conditions. The square terms of aging temperature and aging time were insignificant ($P_{Value} > 0.05$) on the specific surface areas. However, both square terms of aging temperature and time are shown in
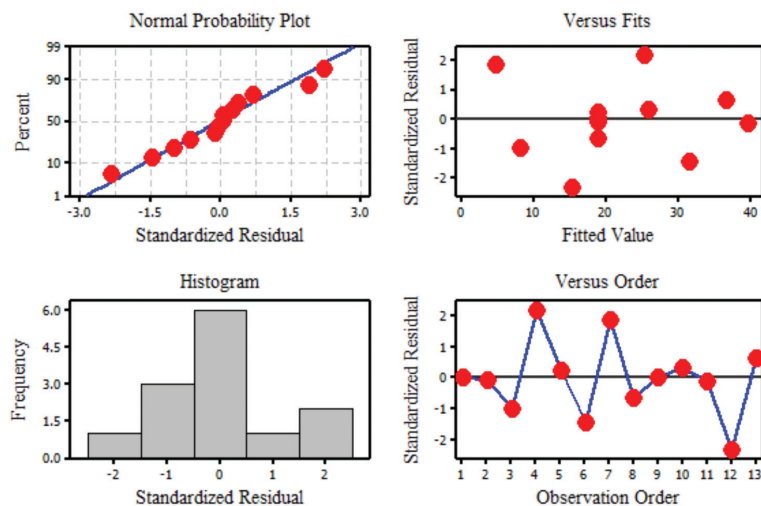

FIGURE 3. Residual plot for specific surface area

versus the order. The points in the normal probability plot are relatively straight and histogram plot appeared to be normally distributed. Residuals against fitted values and observation order display the general random suggesting the relationship in linear is possible. Based on these results, the error of experiment was not observed in every run indicating the same trends with other researches (Krasae & Wantala 2015; Suwannaruang et al. 2015; Yodsa-nga et al. 2015).

Comparison of the experimental results with the predicted results is shown in Figure 4. R^2 and R^2_{adj} were about 88.94% and 77.61%, respectively. A large different value between R^2 and R^2_{adj} suggested that the insignificant terms cannot be negligible or removed from full quadratic equation.
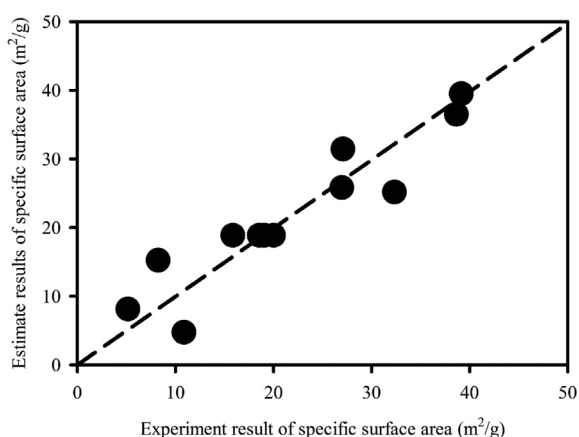

FIGURE 4. Experimental and estimated results for specific surface area (m^2/g)

The ANOVA results are displayed in Table 4. The results can confirm the precision of predicted equation by using 95% confidence. The regression term was significant ($P_{Value} < 0.05$) due to F_{Value} (9.32) was higher than $F_{Critical}$ ($F_{(0.05,5,7)} = 3.97$). The main effect term was significant proven by F_{Value} (20.56) higher than $F_{Critical}$ ($F_{(0.05,2,7)} = 4.74$), while the square and interaction terms were insignificant terms ($F_{Value} < F_{Critical}$). Lack of fit (LOF) term was considered. F_{Value} (23.25) of LOF term was higher than $F_{Critical}$ ($F_{(0.05,3,4)} = 6.59$) and P_{Value} about 0.005 ($P_{Value} < 0.05$), which can be said that the lack of fit of predicted results calculated from (2) was significant. However, showing of high value for R^2 correlation between predicted results and experiment results, (2) might be used to compute the specific surface area in effect of hydrothermal conditions to calculate the specific surface areas of Na-P1 samples.

Figures 5 and 6 show the main and interaction plots of aging temperature and time, respectively. The specific surface area sharply decreased with increasing of aging temperature from 105ºC to 150ºC then stable up to 195ºC, whereas the specific surface area sharply decreased with increasing of aging time from 12 to 84 h, as shown in Figure 5.

The surface and contour plots as shown in Figure 6(a)-6(b) obviously show the same trend with the main effect plot because of the insignificant of interaction in both terms. The lowest aging temperature (105ºC) and aging time (12 h) gave the highest specific surface area as about 46 m^2/g computed by (2). The replication of zeolite synthesis was conducted in three times at the maximal specific surface area condition. The results of XRD

TABLE 4. ANOVA for specific surface area

Source	DF	F-value	P-value	
Regression	5	9.32	0.005	Significant
Linear	2	20.56	0.001	Significant
Temperature	1	21.39	0.002	Significant
Time	1	19.73	0.003	Significant
Square	2	2.28	0.172	Insignificant
Temperature * Temperature	1	4.54	0.071	Insignificant
Time * Time	1	0.05	0.824	Insignificant
Interaction	1	0.92	0.370	Insignificant
Temperature * Time	1	0.92	0.370	Insignificant
Residual error	7			
Lack-of-fit	3	23.25	0.005	Significant
Pure error	4			
Total	12			

Fisher's F test (F_{value}) at 95% confidence ($\alpha = 0.05$)

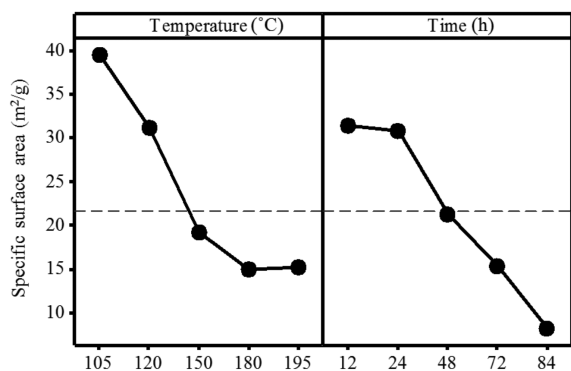| Source	DF1	DF2	$F_{critical}$
$F_{(0.05,DF1,DF2)}$	5	7	3.97
$F_{(0.05,DF1,DF2)}$	2	7	4.74
$F_{(0.05,DF1,DF2)}$	1	7	5.59
$F_{(0.05,DF1,DF2)}$	3	4	6.59

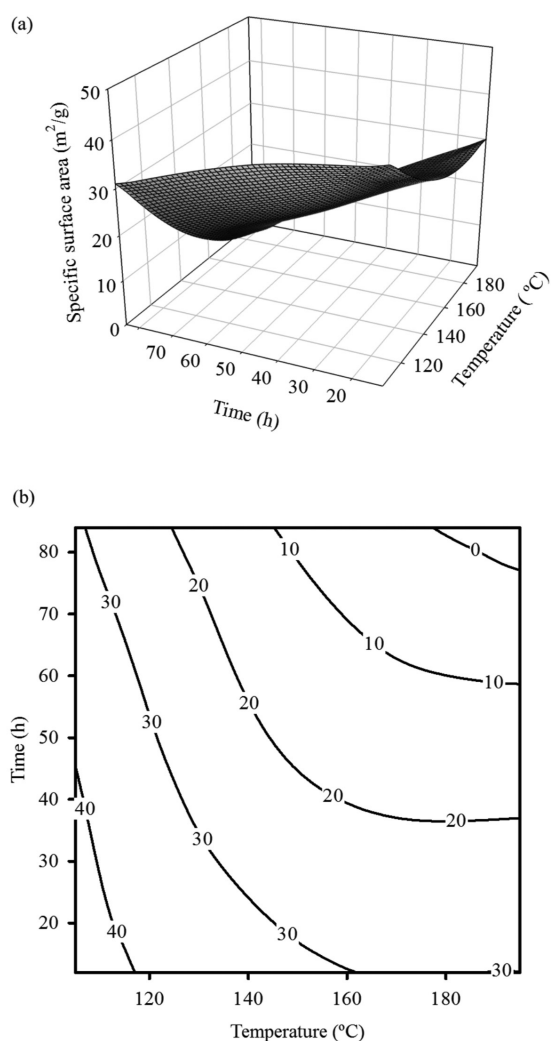FIGURE 5. Trends of specific surface area for varying aging temperatures and times

(a)

(b)

FIGURE 6. Surface plot (a) and contour plot (b) of specific surface area

patterns in triplicate of synthesized Na-P1 samples are displayed in Figure 7. The results of the specific surface area were about 75.17, 61.38 and 71.45 m²/g, which are higher than the calculated results related to significant LOF terms. Thus, the suitable condition to prepare Na-P1 by hydrothermal process from MFA was 105ºC of aging temperature and 12 h of aging time.

Finally, the chemical compositions of MFA and Na-P1 were examined by X-ray fluorescence as shown in Table 5. The mass ratios of SiO_2/Al_2O_3 of MFA and Na-P1 were about 1.77 and 1.90, respectively. Moreover, this research successfully synthesized a slightly pure Na-P1 in high content of ferric oxide (Fe_2O_3) which was 12 percent weight higher than the one in coal fly ash. However, this finding differs from some published studies (Adamczyk & Bialecka 2005). The specific surface areas not only depended on aging temperature and time in hydrothermal process for Na-P1 synthesis but also other independent effects such as SiO_2/Al_2O_3 ratio and NaOH concentration were significantly shown on specific surface areas comparing results as shown in Table 6. Interestingly, the specific surface area prepared by hydrothermal technique showed the higher value (69.33±7.95 m²/g) than other researches at aging temperature of 105ºC, aging time of 12 h without adding any alumina and silica sources at mass ratio of SiO_2/Al_2O_3 about 1.77 and NaOH concentrations of 2.8 molar (Izidoro et al. 2012; Rongsayamanont & Sopajaree 2007).
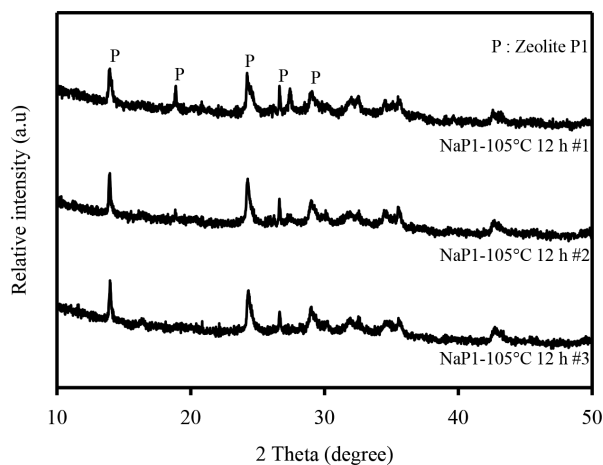

FIGURE 7. Synthesized Na-P1 at 105ºC and 12 h for 3 replications

TABLE 5. Composition (wt. %) of fly ash and synthesized zeolite P1 from Mae Moh fly ash

Components	SiO₂	Al₂O₃	CaO	Fe₂O₃	K	Mg	Na
Fly ash	35.15	19.89	20.11	12.73	2.89	2.02	1.91
Na-P1	32.35	17.00	22.30	16.55	0.58	1.33	7.82

TABLE 6. Comparing Na-P1 with other researches by alkaline hydrothermal treatment from fly ash

SiO_2/Al_2O_3 mass ratio	Aging temperature (°C)	Aging time (h)	NaOH concentration (molar)	Specific surface area (m²/g)	References
1.30	120	4	5.53	-	(Kazemian et al. 2010)
1.76, 2.72	100	24	3.5	56.70	(Izidoro et al. 2012)
1.42	120-320	6	1.16	-	(Adamczyk & Bialecka 2005)
1.79	110	96	1	56.17	(Rongsayamanont & Sopajaree 2007)
2.02, 2.64	90	24	1	-	(Moutsatsou et al. 2006)
1.77	105	12	2.8	69.33±7.95	Present study

CONCLUSION

The Na-P1 mixed with an alkaline solution was successfully synthesized by hydrothermal method. The crystallinity of Na-P1 increased with increasing of aging temperature and time, whereas the specific surface area shows an opposite tendency with crystallinity. In mathematical model, the aging temperature and time in the main effect terms (X_1 and X_2) were found to be a significant negative effect ($P_{Value} < 0.05$) to the specific surface area, while the interaction term of aging temperature and time (X_1X_2) was not statistically significant. The conditions resulting in the maximum specific surface area (46 m²/g from the computed result and 69.33±7.95 m²/g from experimental result) were aging temperature of 105°C and aging time of 12 h. Despite these promising results, further work is required to use the synthesized Na-P1 as a support material of Cu-Fe in Fenton-like process.

REFERENCES

Adamczyk, Z. & Bialecka, B. 2005. Hydrothermal synthesis of zeolites from polish coal fly ash. *Polish Journal of Environmental Studies* 14(6): 713-719.

Belviso, C., Giannossa, L.C., Huertas, F.J., Lettino, A., Mangone, A. & Fiore, S. 2015. Synthesis of zeolites at low temperatures in fly ash-kaolinite mixtures. *Microporous and Mesoporous Materials* 212: 35-47.

Bukhari, S.S., Behin, J., Kazemian, H. & Rohani, S. 2015. Conversion of coal fly ash to zeolite utilizing microwave and ultrasound energies: A review. *Fuel* 140: 250-266.

Cama, J., Ayora, C., Querol, X. & Ganor, J. 2005. Dissolution kinetics of synthetic zeolite NaP1 and its implication to zeolite treatment of contaminated waters. *Environmental Science & Technology* 39(13): 4871-4877.

Cardoso, A.M., Horn, M.B., Ferret, L.S., Azevedo, C.M.N. & Pires, M. 2015. Integrated synthesis of zeolites 4A and Na-P1 using coal fly ash for application in the formulation of detergents and swine wastewater treatment. *Journal of Hazardous Materials* 287: 69-77.

Grela, A., Hebda, M., Łach, M. & Mikuła, J. 2016. Thermal behavior and physical characteristics of synthetic zeolite from CFB-coal fly ash. *Microporous and Mesoporous Materials* 220: 155-162.

Izidoro, J.C., Fungaro, D.A., Santos, F.S. & Wang, S. 2012. Characteristics of Brazilian coal fly ashes and their synthesized zeolites. *Fuel Processing Technology* 97: 38-44.

Kazemian, H., Naghdali, Z., Kashani, T.G. & Farhadi, F. 2010. Conversion of high silicon fly ash to Na-P1 zeolite: Alkaline fusion followed by hydrothermal crystallization. *Advanced Powder Technology* 21(3): 279-283.

Krasae, N. & Wantala, K. 2015. Enhanced nitrogen selectivity for nitrate reduction on Cu-nZVI by TiO_2 photocatalysts under UV irradiation. *Applied Surface Science* 380: 309-317.

Ma, X., Zhang, Z. & Wang, A. 2016. The transition of fly ash-based geopolymer gels into ordered structures and the effect on the compressive strength. *Construction and Building Materials* 104: 25-33.

Moutsatsou, A., Stamatakis, E., Hatzitzotzia, K. & Protonotarios, V. 2006. The utilization of Ca-Rich and Ca–Si-Rich fly ashes in zeolites production. *Fuel* 85(5-6): 657-663.

Murayama, N., Yamamoto, H. & Shibata, J. 2002. Mechanism of zeolite synthesis from coal fly ash by alkali hydrothermal reaction. *International Journal of Mineral Processing* 64(1): 1-17.

Okoye, F.N., Durgaprasad, J. & Singh, N.B. 2015. Mechanical properties of alkali activated flyash/kaolin based geopolymer concrete. *Construction and Building Materials* 98: 685-691.

Onutai, S., Jiemsirilers, S., Thavorniti, P. & Kobayashi, T. 2015. Aluminium hydroxide waste based geopolymer composed of fly ash for sustainable cement materials. *Construction and Building Materials* 101: 298-308.

Phoo-Ngernkham, T., Sata, V., Hanjitsuwan, S., Ridtirud, C., Hatanaka, S. & Chindaprasirt, P. 2015. High calcium fly ash geopolymer mortar containing Portland cement for use as repair material. *Construction and Building Materials* 98: 482-488.

Pimraksa, K., Chindaprasirt, P. & Setthaya, N. 2010. Synthesis of zeolite phases from combustion by-products. *Waste Management and Research* 28(12): 1122-1132.

Rongsayamanont, C. & Sopajaree, K. 2007. Modification of synthetic zeolite pellets from lignite fly ash A: The pelletization. In *World of Coal Ash (WOCA)*. pp. 1-9. Northern Kentucky, USA. http://www.flyash.info/2007/12rongsay.pdf.

Sang, S., Liu, Z., Tian, P., Liu, Z., Qu, L. & Zhang, Y. 2006. Synthesis of small crystals zeolite NaY. *Materials Letters* 60(9-10): 1131-1133.

Suwannaruang, T., Rivera, K.K.P., Neramittagapong, A. & Wantala, K. 2015. Effects of hydrothermal temperature and time on uncalcined TiO_2 synthesis for reactive Red 120 photocatalytic degradation. *Surface and Coatings Technology* 271: 192-200.

Thuadaij, P. & Nuntiya, A. 2012. Effect of the SiO_2/Al_2O_3 Ratio on the synthesis of Na-X zeolite from Mae Moh fly ash. *ScienceAsia* 38(3): 295-300.

Volli, V. & Purkait, M.K. 2015. Selective preparation of zeolite X and A from flyash and its use as catalyst for biodiesel production. *Journal of Hazardous Materials* 297: 101-111.

Wei, N., Wang, X. & Guan, W. 2015. Synthesis of pure zeolite from coal fly ash for ammonium removal. *Chinese Journal of Environmental Engineering* 9(2): 795-799.

Yodsa-nga, A., Millanar, J.M., Neramittagapong, A., Khemthong, P. & Wantala, K. 2015. Effect of manganese oxidative species in as-synthesized K-OMS 2 on the oxidation of benzene. *Surface and Coatings Technology* 271: 217-224.

Zhang, X., Tang, D., Zhang, M. & Yang, R. 2013a. Synthesis of NaX zeolite: Influence of crystallization time, temperature and batch molar ratio SiO_2/Al_2O_3 on the particulate properties of zeolite crystals. *Powder Technology* 235: 322-328.

Zhang, Z., Li, J., Li, H., Wang, H., Zhu, J. & He, Q. 2013b. Dynamic formation of zeolite synthesized from fly ash by alkaline hydrothermal conversion. *Waste Management and Research* 31(11): 1160-1169.

W. Chansiriwat, D. Tanangteerapong & K. Wantala*
Department of Chemical Engineering
Faculty of Engineering, Khon Kaen University
Khon Kaen 40002
Thailand

W. Chansiriwat & K. Wantala*
Chemical Kinetics and Applied Catalysis Laboratory (CKCL)
Faculty of Engineering, Khon Kaen University
Khon Kaen 40002
Thailand

K. Wantala*
Research Center for Environmental and
Hazardous Substance Management (EHSM)
Faculty of Engineering, Khon Kaen University
Khon Kaen 40002
Thailand

*Corresponding author; email: kitirote@kku.ac.th